Molecular-dynamics study of lattice vibrations in the mixed crystal $K_{0.5}Rb_{0.5}Cl$

E. Roger Cowley
Department of Physics, Camden College of Arts and Sciences, Rutgers—The State University, Camden, New Jersey 08102-1205

Michael L. Klein
Department of Chemistry, University of Pennsylvania, Philadelphia, Pennsylvania 19104-6323
(Received 22 October 1990; revised manuscript received 4 March 1991)

We have performed molecular-dynamics simulations on a system of 512 ions arranged on a sodium chloride lattice, consisting of 256 chlorine ions, and a random mixture of 128 potassium ions and 128 rubidium ions, interacting through Coulombic and short-range rigid-ion potentials. Results are presented for the scattering function $S(\mathbf{Q},\omega)$ for a range of wave vectors, and for the Fourier-transformed velocity-velocity autocorrelation function. Peaks in the scattering function for the mixture are broader than those of pure KCl and are in some cases split.

I. INTRODUCTION

The vibrational properties of mixed crystals of alkali halides have been widely studied experimentally by both optical methods[1–3] and neutron inelastic scattering.[4–6] The optical measurements give results primarily for the long-wavelength modes of vibrations. The results for a large number of alkali halides and other diatomic materials have led to a classification of the compounds into one- and two-mode materials. In the one-mode case the system appears to show a single infrared absorption mode, whose frequency changes smoothly as the proportions of the mixture change, from the value appropriate to one pure substance to the value measured for the other pure substance. In two-mode materials there appear to be two resonance frequencies, at frequencies close to those of the two pure materials. Neutron-scattering measurements can explore the whole Brillouin zone, but the results currently available are more limited. A preliminary study on potassium-rubidium bromide[4] was remarkable mainly for a strong resonance in one of the acoustic branches. The present calculation shows a somewhat similar behavior. More complete data are now available for potassium-rubidium iodide,[5] potassium-rubidium chloride, and potassium-chloride bromide.[6] Interestingly, in the last work, the authors found qualitatively similar results for all materials, even though potassium-rubidium chloride is classified optically as a one-mode material, while potassium-rubidium iodide is two mode. In all cases many of the peaks in the scattered neutron intensity were split into two. It should be noted though that they were also broadened and of low intensity so that they were not well defined. In our results we find a small number of peaks which are clearly double, but many which are extremely broad and deformed.

The theoretical analysis of the long-wavelength optical modes has been mainly through empirical models, especially the modified random-element isodisplacement model.[2,7] Several criteria have been proposed to predict whether a material should show one- or two-mode behavior.[8] These calculations are not capable of giving detailed predictions of line shapes or of dispersion relations. Taylor[9] has applied the coherent-potential approximation to the alkali halides. This is, in principle, a more fundamental and complete approach, but so far numbers have been obtained only for the long-wavelength modes and including only mass disorder.

The molecular-dynamics technique is ideally suited to the study of disordered crystals, since the method makes no use of the periodicity of the perfect structure. The calculation for a discorded crystal is no more demanding than that for an ordered crystal. It is also the only technique which yields results for the scattering function $S(\mathbf{Q},\omega)$ which are exact within the, admittedly large, numerical uncertainties. Jacucci, Klein, and Taylor[10] have used the method to study an alloy of potassium in rubidium metal, and there have been studies of structural transformations in mixed cyanides[11] and of the glass transition in potassium-calcium nitrates.[12] We apply the technique here to a rigid-ion model of $K_{0.5}Rb_{0.5}Cl$, which is one of the crystals studied by Beg and Kobbelt.[6] Because of the use of the rigid-ion model, the calculated frequencies cannot be expected to agree well with experiment. Nevertheless, our results will show the type of behavior to be expected of a generic mixed alkali halide, and this should be of value to future experimental investigations.

II. DETAILS OF THE MODEL

In setting up the computer program, we wished to use a model which could be applied to a variety of mixed alkali halide crystals. There have been several attempts to derive families of interatomic potentials, notable by Fumi and Tosi,[13] Sangster and Dixon,[14] and Catlow, Diller, and Norgett.[15] The latter two investigations obtained shell parameters for the polarizable ions, but in the work of Catlow, Diller, and Norgett the interatomic potentials were determined first, from the structural and elastic properties, and the shell-model parameters then chosen to fit the optical and dielectric properties. In the present

work we have used only a rigid-ion formalism, though we aim to extend the calculations to a shell model in the near future. For the interactions between like ions, and between alkali and halogen ions, we have used model 2 of Catlow, Diller, and Norgett. In this model the interactions between positive and negative ions are written in the Born-Mayer form, while the interactions between like ions are exponential at short distances and $1/r^6$ at large distances, with two regions represented by polynomials in between. The formal ionic charges of $\pm e$ were used. We can expect this model to give a good description of the elastic properties, but the optical frequencies are left to fall where the rigid-ion model leaves them. Typically, this means that the longitudinal-optic branches are too high, and in pure KCl the LA branch in the [100] direction does not have the correct shape. The quasiharmonic dispersion curves for the model of pure KCl are shown as solid lines in Fig. 1 for the two principal symmetry directions. Also shown are the experimental curves[16] as dashed lines and, as dots, the centers of the peaks in $S(\mathbf{Q},\omega)$ found in the molecular-dynamics calculation, which was at 300 K. It can be seen that for the acoustic branches and transverse-optic branch the frequencies are barely shifted at room temperature from the quasiharmonic values. For the longitudinal-optic branch, the shifts are noticeable, and as will be shown later, the peaks are also broadened.

For the mixed crystal we also require potentials between ions of different species on the same sublattice, that is, between the potassium and rubidium ions in the present case. In the rigid-ion approximation the Coulomb interactions between both species of positive ion are the same, but for the short-range terms we have to resort to general ideas regarding such mixed interactions.[17] The parameters A and C of the interaction are approximated by the geometric average of the interactions for the two separate ions, and the parameters ρ, r_a, r_b, and r_m are approximated by algebraic means. This type of approximation has not worked well in situations where it has been carefully tested,[18,19] but it seems to be the best we can do at the present. In the present application the largest second-neighbor interaction is in the chlorine sublattice, which is not disordered, and the uncertainty in the potassium-rubidium interaction is unlikely to matter.

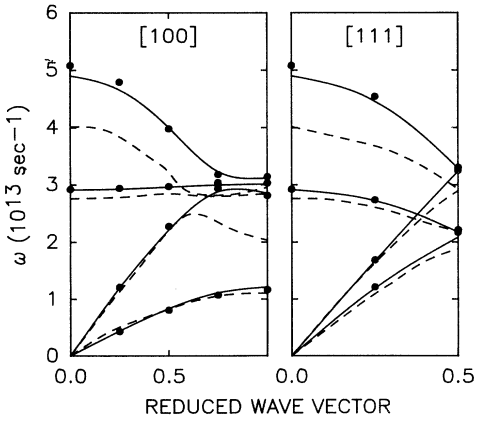

FIG. 1. Dispersion relations in the [100] and [111] directions for pure KCl. Dashed lines are experimental results, solid lines are quasiharmonic calculations for the rigid ion model, and dots are the center of peaks in $S(\mathbf{Q},\omega)$.

III. MOLECULAR-DYNAMICS TECHNIQUE

The general features of the molecular-dynamics method have been described by Allen and Tildesley.[20] We performed molecular-dynamics runs for two systems, each consisting of a cube of 512 ions, as well as a number of runs with smaller samples. One system was a crystal of pure KCl with nearest-neighbor distance r_0, of 3.116Å. The other had equal numbers of potassium and rubidium ions randomly positioned on the positive-ion sublattice, with a nearest-neighbor distance of 3.1875Å, which is the mean of the values for pure KCl and pure RbCl. The ions were initially at their equilibrium positions in the pure crystal, with a distribution of velocity components such that the center of mass was stationary and the sum of the kinetic energies was equal to the expected internal energy of the crystal at the desired temperature of 300 K. For the alkali halides this is very close to the equipartition value so that only one adjustment of the energy was required in each case. The equations of motion for the sample were integrated using the velocity-Verlet algorithm[20] with a time step of 0.01 ps. The first 500 time steps were discarded. The kinetic and potential energies and pressure had stabilized by this time. For both samples the pressure was zero within the statistical uncertainty. The equations of motion were then integrated for a further 10 000 time steps, while the positions and velocities were recorded every other time step for later analysis. The temperatures of the two samples over the complete runs were 299.0 and 299.4 K, respectively. During the equilibrating period, the ions also adjust their average positions to correspond to the disordered material. The calculation of the forces, including the Coulomb contributions, is carried out exactly for the actual positions of the ions.

The short-range forces were included for all neighbors with equilibrium separations up to $3r_0$, and the electrostatic forces were evaluated using the Ewald technique. It now seems established[21,22] that the well-known expression for the electrostatic energy as sums over neighbors in real space and over reciprocal lattice vectors is complete only if the surface of the sample is covered with a conducting layer. For a specimen in vacuum there is an additional term, depending on the instantaneous dipole moment of the specimen and the shape-dependent depolarization factors. In an earlier molecular-dynamics simulation of pure sodium chloride,[23] we omitted this term and, as a consequence, obtained a triply degenerate optical frequency at $q=0$ corresponding to the transverse-optic mode. It is known[24] that, for wavelengths which are small compared with the size of the specimen and compared with the wavelength of light of the same frequency, the longitudinal-optic branch has a frequency which is substantially raised above that of the transverse-optic

branch by the presence of a macroscopic electric field. In lattice-dynamics calculations using the Ewald transformation, the term corresponding to the macroscopic electric field can be identified, and it is common practice in calculations for long wavelenghts to take the limiting behavior of this term. In order to have a mode at $q=0$ which connects smoothly with the LO branch, we can choose a sample shape such that the depolarizing field reproduces this macroscopic field. In particular, we choose a slab cut perpendicular to the x direction. There is then an additional force in the x direction acting on each ion, proportional to the x component of the instantaneous dipole moment. The only disadvantage to this procedure is that the sample no longer has cubic symmetry with respect to the $q=0$ modes. The mean-square displacement in the x direction, for example, is slightly different from the mean-square displacements in the y and z directions, though the difference is small.

The main effort of our subsequent analysis of the position and velocity file was in the evaluation of a neutron-scattering-length weighted correlation function

$$F(\mathbf{Q},t)=\langle \rho(\mathbf{Q},t)\rho^*(\mathbf{Q},0)\rangle \ ,$$

$$\rho(\mathbf{Q},t)=\sum_i b_i \exp(i\mathbf{Q}\cdot\mathbf{R}_i) \ ,$$

where b_i is the scattering length for the particular nuclear species. The sum is over all the ions in the sample, and the components of the wave vector $\mathbf{Q}$ are restricted to integer multiples of $\pi/4r_0$. From $F(\mathbf{Q},t)$ the scattering function can be calculated as a Laplace-Fourier transform:

$$S(\mathbf{Q},\omega)=\int_0^\infty F(\mathbf{Q},t)\exp(i\omega t)dt \ .$$

The advantage of this two-step procedure is that the noise level in the results can be recognized fairly readily. For small values of t, $F(\mathbf{Q},t)$ is well defined, but at some point it behaves erratically. Typically, $F(\mathbf{Q},t)$ looks like a damped oscillator function for small times, but the amplitude eventually stops decreasing. Our procedure was to multiply the calculated correlation function by a Gaussian function $\exp(-\alpha t^2)$ with α chosen so that the Gaussian had fallen to half-height at the time where $F(\mathbf{Q},t)$ appeared to be unreliable. In the worst case this time was 8 ps. Averaging $F(\mathbf{Q},t)$ over several equivalent wave vectors pushed the divergent behavior to later time values. In the most favorable cases the correlation functions appeared reliable to more than 30 ps.

In the important cases where $\mathbf{Q}$ is a reciprocal lattice vector, $F(\mathbf{Q},t)$ contains a very large contribution from the Bragg peak. While this is independent of time and should not affect $S(\mathbf{Q},\omega)$ at finite frequencies, in practice the inelastic contribution can be lost in the rounding error. In those cases we calculated the one-phonon contribution to $F(\mathbf{Q},t)$, obtained by expanding $\rho(\mathbf{Q},t)$ in powers of the displacements of the ions from their equilibrium positions and retaining only the linear term.

A second useful quantity to calculate is a mass-weighted velocity-velocity autocorrelation function:

$$G(t)=\sum_i m_i\langle \mathbf{v}_i(t)\cdot\mathbf{v}_i(0)\rangle \ .$$

For a harmonic crystal the frequency distribution function, $g(\omega)$ is given by

$$g(\omega)=\frac{2}{\pi kT}\int_0^\infty G(t)\cos(\omega t)dt \ , \quad (1)$$

and in view of the agreement between the quasiharmonic frequencies and the center of the neutron-scattering peaks, we can expect that the molecular-dynamics results will be close to the harmonic behavior.

IV. RESULTS

Figure 2(a) shows a typical result for the scattering-length-weighted $F(\mathbf{Q},t)$ calculated for the pure KCl crystal. In all figures the wave-vector components are given in units of $\pi/4r_0$. The wave vector (2,0,0) is half-way to the zone boundary, and in this case we have averaged over three equivalent wave vectors. The dominant contribution at this wave vector is from the longitudinal-acoustic phonon. The curve for the pure crystal shows a nearly perfect damped oscillator form over a time range of about 12 ps. Figure 2(b) shows $F(\mathbf{Q},t)$ for the same wave vector in the mixed crystal. The oscillation is much more heavily damped. This is not a typical result, but is one of the most heavily damped acoustic peaks we located. Note also that the oscillation does not decay to zero in this case, but to a finite value. This is caused by the disorder of the scattering lengths in the crystal, which gives rise to incoherent elastic scattering between the Bragg peaks.

The corresponding peaks in $S(\mathbf{Q},\omega)$ are shown in Fig. 3, which also shows the results for the transverse acoustic mode. Figures 3(a) and 3(b) show the transverse and longitudinal peaks in the pure crystal. Both are very sharp.

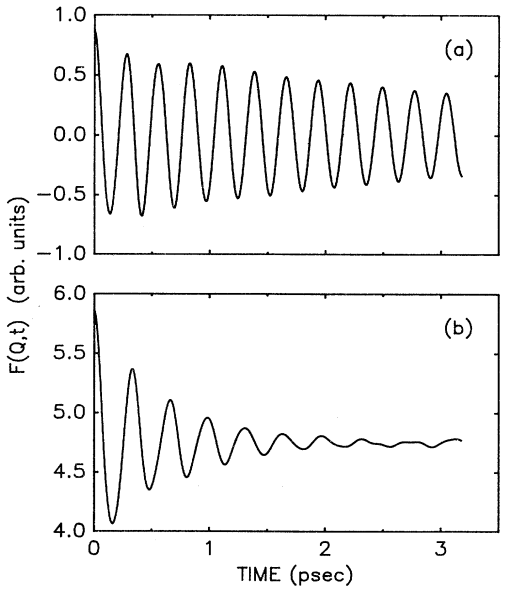

FIG. 2. Scattering-length-weighted correlation function $F(\mathbf{Q},t)$ for the wave vector (2,0,0). (a) Pure KCl and (b) mixed crystal $K_{0.5}Rb_{0.5}Cl$.

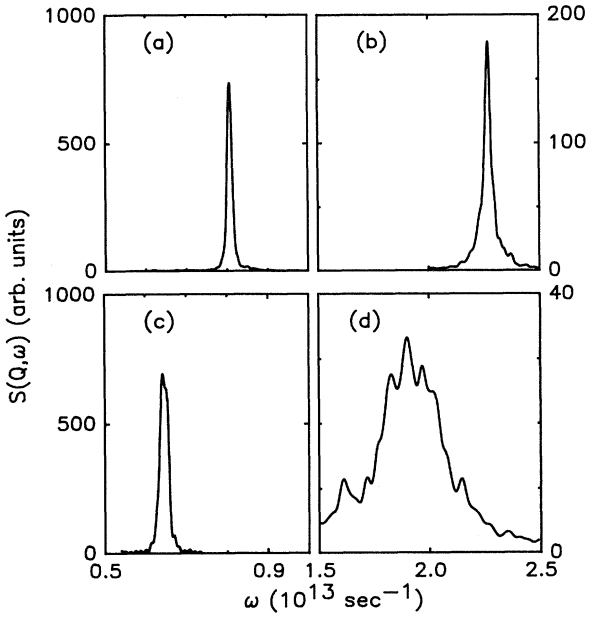

FIG. 3. $S(\mathbf{Q},\omega)$ for acoustic modes at reduced wave vector (2,0,0). (a) and (b) are T and L modes for the pure crystal; (c) and (d) are for the mixed crystal.

Figures 3(c) and 3(d) show the corresponding peaks for the disordered crystal. The transverse peak is shifted downward in frequency, which is to be expected since the average mass of the metal ions has been increased, and it shows a small increase in width. The longitudinal-acoustic mode is also shifted downward and has a dramatic increase in width. We interpret this as a resonance phenomenon, similar to the one reported by Buyers and Cowley.[4]

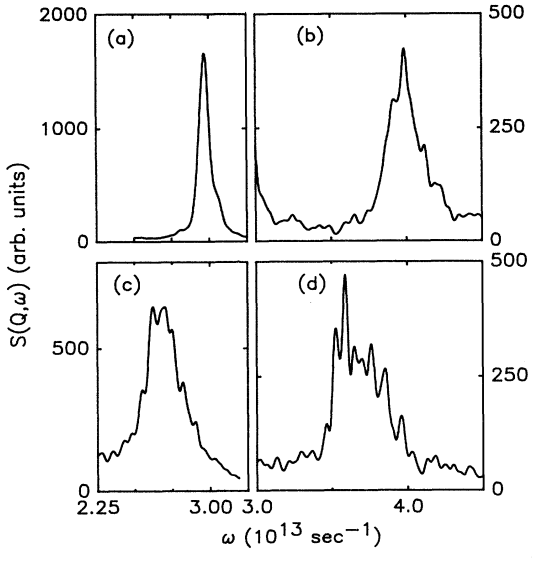

FIG. 4. $S(\mathbf{Q},\omega)$ for optical modes at reduced wave vector (2,0,0). (a) and (b) are T and L modes for the pure crystal; (c) and (d) are for the mixed crystal.

Figure 4 shows the corresponding results for the optical modes at the same reduced wave vector. The pure crystal modes are shown in Figs. 4(a) and 4(b), and the disordered crystal modes in Figs. 4(c) and 4(d). Both of the optical modes in the pure crystal show some broadening, caused by anharmonicity. In the disordered crystal the modes are again shifted downward and further broadened. The vertical scales are arbitrary, but are consistent for a given branch, so that the peak height for the TO mode is reduced by about a factor of 3 in the disordered crystal. Also, the same smoothing procedure has been used for both crystals, but the peaks for the disordered crystal seem to be more jagged.

The modes corresponding to the zone boundary in the [111] direction, a reduced wave vector of (2,2,2) in the present units, are of special interest. In a quasiharmonic calculation for the ordered crystal, only one atomic species vibrates in each mode. For plausible force models, in both KCl and RbCl the light chlorine ions vibrate in the optical modes and the alkali metal vibrates in the acoustic modes. If the masses of the alkali ions are disordered but not the force constants, the optical modes should be unaffected since the disordered ions are not vibrating. The peak in the scattering function should thus be sharp. Any broadening of the peak arises from force constant disorder or anharmonicity. The results for the scattering function are shown by the solid lines in Fig. 5(a) for the transverse modes, at a wave vector of (6,6,10),

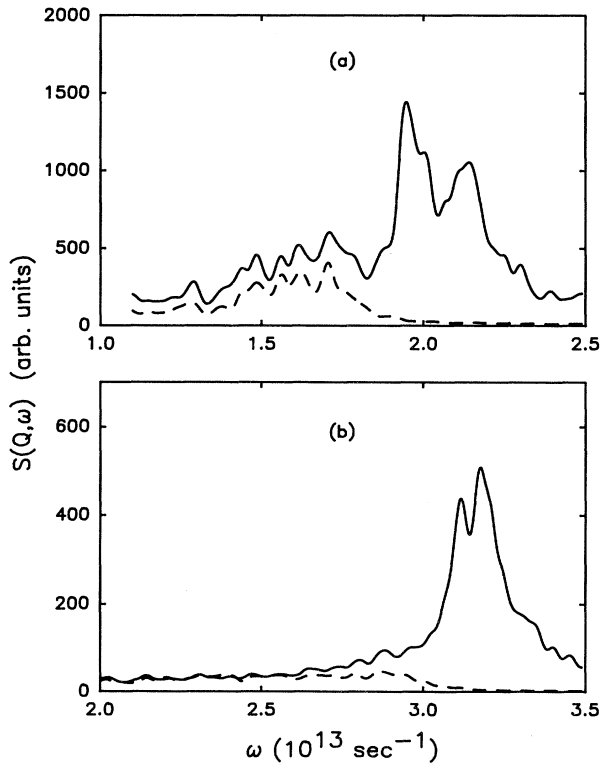

FIG. 5. $S(\mathbf{Q},\omega)$ for the [111] zone boundary. (a) Transverse modes and (b) longitudinal modes. Dashed lines show the results of setting the Cl scattering length to zero.

and in Figure 5(b) for the longitudinal modes,, at a wave vector of (6,6,6). In each case there is a double peak. A complication is that the separation of the acoustic and optical frequencies is very small in pure KCl. However, we can clarify the theoretical results by repeating the calculations with the chlorine scattering length set to zero. These results are shown by the dashed lines in the figure. It appears that the double peaks are chlorine vibrations to be associated with the optical modes, while the acoustic modes have been degraded into a low, broad maximum in the transverse case, and there is no identifiable peak for the longitudinal-acoustic mode.

The optical modes at the zone center are also especially interesting since they are accessible by optical measurements. Figures 6(a) and 6(b) show the transverse- and longitudinal-optic modes for pure KCl, and Figs. 6(c) and 6(d) show the results for the mixed crystal. In all cases the one-phonon approximation is used. The transverse peak in the mixed crystal shows some evidence of splitting, while the corresponding peak for the pure crystal is well shaped. The LO mode at the zone center is the highest-frequency mode in the crystal and is also the mode most strongly affected by anharmonicity.[25] Our result for the pure crystal is unusual. The secondary peaks at frequencies below the main peak are not a result of the damping procedure used. We have tried a variety of damping and truncation techniques and find that these peaks persist. They may, however, be a consequence of the small sample size used. In the mixed crystal the peak shows the additional broadening due to disorder.

The neutron-scattering study on $K_{0.5}Rb_{0.5}Cl$ showed a double peak for the TO mode,[6] while it is observed optically to be single.[1] In an attempt to resolve this question, we also calculated the Fourier transform of the autocorrelation function of the dipole moment of the sample. This is, in fact, very similar to the calculation of $S(\mathbf{Q},\omega)$ in the one-phonon approximation, except that the ionic displacements are weighted by the charges instead of by the scattering lengths. The resulting curve for the mixed crystal, shown in Fig. 7, is quite similar to the neutron-scattering peak in Fig. 6(c). It shows a considerable width and some suggestion of splitting. Whether this would be interpreted as one- or two-mode behavior is not clear.

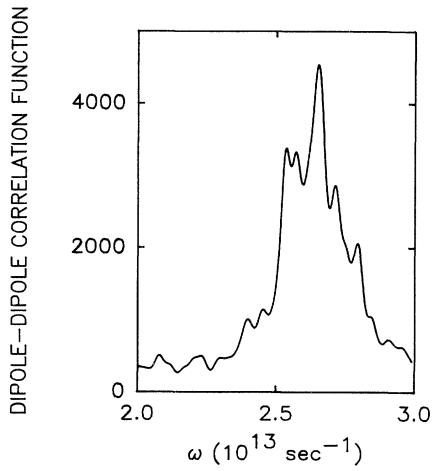

FIG. 7. Fourier transform of the autocorrelation function of the sample dipole moment.

Because of the restricted set of wave vectors accessible to us, we cannot make a detailed comparison with many of the neutron groups shown by Beg and Kobbelt.[6] They do give a well-defined result for the transverse-optic mode at a reduced wave vector $(\pi/r_0)(0.7,0.7,0)$, and we can get close to this. Figure 8(a) shows the experimental re-

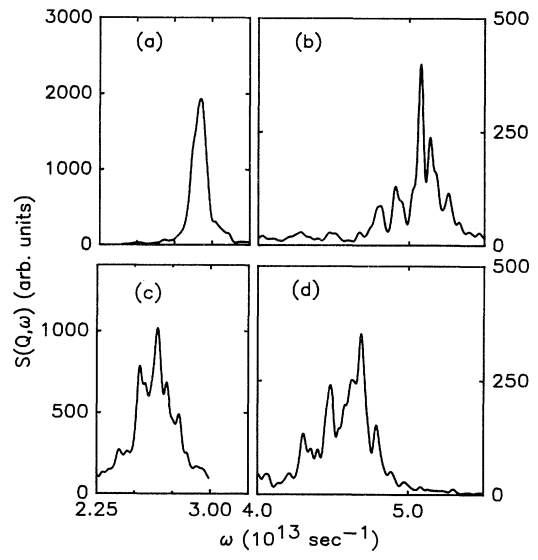

FIG. 6. $S(\mathbf{Q},\omega)$ for zone-center optical modes. (a) and (b) are TO and LO modes for the pure crystal; (c) and (d) are for the mixed crystal. A one-phonon approximation was used.

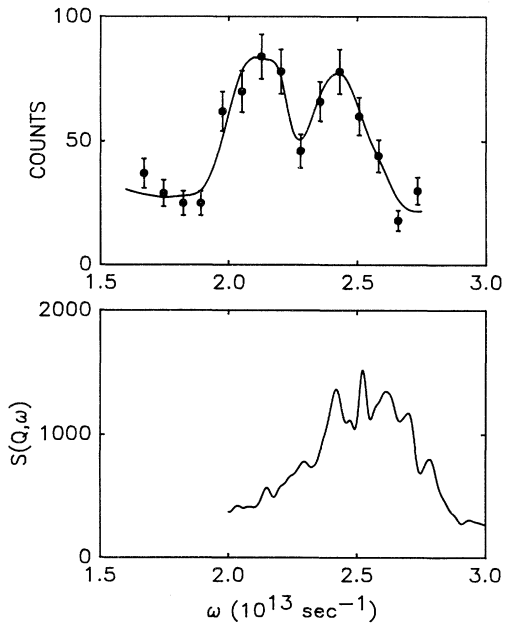

FIG. 8. Comparison of the experimental TO neutron group at a reduced wave vector of $(\pi/r_0)(0.7,0.7,0)$ with $S(\mathbf{Q},\omega)$ calculated for a reduced wave vector of $(\pi/r_0)(0.75,0.75,0)$.

sult, and Fig. 8(b) shows the calculate curve at a wave vector (13,19,0), which corresponds to a reduced wave vector of $(\pi/r_0)(0.75,0.75,0)$. The calculated peak is centered on too high a frequency, most likely as a consequence of the rigid-ion approximation. The overall width of the peak is in quite good agreement with the measured peak, which contains additional broadening from the instrumental resolution. The calculated peak does not display the dip in the center which Beg and Kobbelt show, but we note that this dip is, in fact, based on a single point and may not actually be so sharp as the line drawn through the points indicates.

Finally, we show in Fig. 9 the results for the frequency distribution function $g(\omega)$ calculated from Eq. (1). Figures 9(b) and 9(c) show the Fourier transforms of the mass-weighted velocity-velocity autocorrelation functions for the ordered and disordered crystals, respectively. To the extent that anharmonic effects are small, these should be close to the distributions of normal-mode frequencies for the two samples. To check this, Fig 9(a) shows a distribution calculated from the quasiharmonic frequencies of the pure sample. To eliminate any differences arising from the smoothing procedure used in the Fourier transforms, each δ-function contribution to the distribution function has been similarly smoothed. It can be seen that the two results for the pure crystal are very similar, except in the highest-frequency range corresponding to the longitudinal-optic branches. Anharmonicity is not negligible in this range. The result [Fig. 9(c)] for the disordered crystal shows a general displacement to lower frequencies, as is to be expected, but also has a rather structureless appearance. We suspect that this is characteristic of a disordered material. An experimental measurement which shows qualitatively similar behavior is the early measurement of incoherent scattering from a Mn-Co alloy by Stewart and Brockhouse.[26]

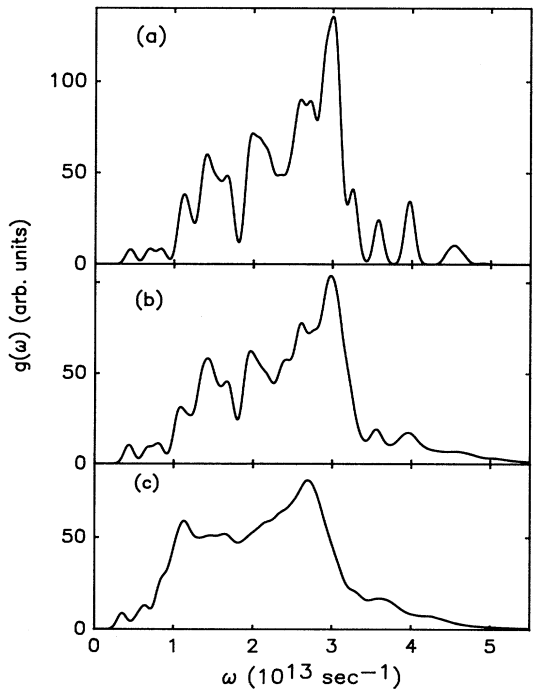

FIG. 9. (a) Density of states calculated or the rigid-ion model of pure KCl. The curve has been convoluted with a Gaussian function corresponding to a decay time of 2 ps. (b) Fourier transform of the mass-weighted velocity-velocity autocorrelation function for the pure KCl crystal. (c) Fourier transform of the mass-weighted veolicty-velocity autocorrelation function for the mixed crystal.

V. DISCUSSION

As a summary of our results and in an attempt to understand them, we plot in Figs. 10 and 11 the central frequencies of the calculated peaks together with bars showing the half-height limits of the peaks. For clarity the transverse and longitudinal modes are shown in separate figures. The dashed lines are the dispersion curves in pure KCl and for pure RbCl, both calculated using the rigid-ion model, at the lattice spacing used for the disordered crystal. For the optical modes the difference between the two curves is quite comparable with the width of the peaks in the disordered crystal, but most of the acoustic modes are sharper than this criterion would indicate. The solid lines are a quasiharmonic virtual crystal calculation, using the averages of the force constants and masses for the two pure crystals. The lines are close to the centers of the peaks in the scattering function with the exception of the longitudinal-optic branch, which has a large upward anharmonic shift, and the longitudinal-acoustic modes in the vicinity of the resonance in the [100] direction.

As far as the distinction between one- and two-mode materials is concerned, our results do make clear that all the optical modes in the disordered material have considerable width. But it seems unlikely to us that a material

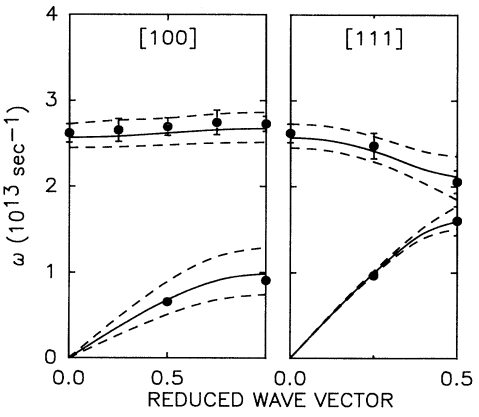

FIG. 10. Frequencies of transverse modes in the two principal symmetry directions. Dots show center of peaks in $S(\mathbf{Q},\omega)$, and error bars show half-height limits. Solid lines are a quasiharmonic virtual crystal calculation, and dashed lines are quasiharmonic frequencies for the two pure crystals.

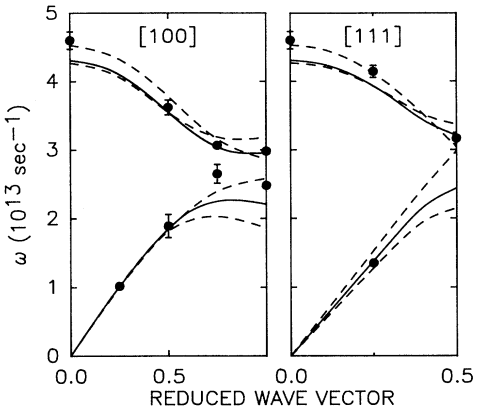

FIG. 11. As in Fig. 10, but for longitudinal modes.

could show two sharp peaks. It is more likely to show a broad peak with a double-hump structure, but this structure could be different, depending on whether the response is probed with light or with neutrons. The division into one- and two-mode materials may be too oversimplified to be useful.

Our calculations were carried out for a sample of 512 ions. This is quite small, and as we indicated earlier, the result for the long-wavelength LO mode in the pure sample may be affected by the small number of modes. However, in most respects our results are qualitatively similar to those we obtained with an even smaller sample, of 216 ions, and are thus a legitimate demonstration of what can be expected of real materials.

In summary, we have used molecular-dynamics calculations to probe the values of dynamical response in mixed alkali halide crystals. Peaks in $S(\mathbf{Q},\omega)$ are broad, even at room temperature, with indications of a structure more complex than with just two or one peaks.

ACKNOWLEDGMENTS

The authors are grateful to Dr. Glenn Martyna for his suggestions. This work was supported by the National Science Foundation under Grant Nos. DMR-8808756, DMR-8819885, and CHE-8722481.

[1]J. H. Fertel and C. H. Perry, Phys. Rev. **184**, 874 (1969).
[2]I. F. Chang and S. S. Mitra, Adv. Phys. **20**, 359 (1971).
[3]I. R. Nair and C. T. Walker, Phys. Rev. B **7**, 2740 (1973).
[4]W. J. L. Buyers and R. A. Cowley, in *Neutron Inelastic Scattering* (IAEA, Vienna, 1968), Vol. 1, pp. 43–46.
[5]J. Aslam, S. Rolandson, M. M. Beg, N. M. Butt, and Q. H. Khan, Phys. Status Solidi B **77**, 603 (1976).
[6]M. M. Beg and M. Kobbelt, Phys. Rev. B **26**, 1893 (1982).
[7]I. F. Chang and S. S. Mitra, Phys. Rev. **172**, 924 (1968).
[8]L. Genzel, T. P. Martin, and C. H. Perry, Phys. Status Solidi B **62**, 83 (1974).
[9]D. W. Taylor, Solid State Commun. **13**, 117 (1973).
[10]G. Jacucci, M. L. Klein, and R. Taylor, Phys. Rev. B **18**, 3782 (1978).
[11]L. J. Lewis and M. L. Klein, Phys. Rev. B **40**, 4877 (1989); **40**, 7080 (1989); **40**, 7904 (1989).
[12]G. F. Signorini, J.-L. Barrat, and M. L. Klein, J. Chem. Phys. **92**, 1294 (1990).
[13]F. G. Fumi and M. P. Tosi, J. Phys. Chem. Solids **25**, 31 (1964); M. P. Tosi and F. G. Fumi, *ibid.*, **25**, 45 (1964).
[14]M. J. L. Sangster and M. Dixon, Adv. Phys. **25**, 247 (1976).
[15]C. R. A. Catlow, K. M. Diller, and M. J. Norgett, J. Phys. C **10**, 1395 (1977).
[16]G. Raunio and L. Almqvist, Phys. Status Solidi **33**, 209 (1969).
[17]J. O. Hirschfelder, C. F. Curtiss, and R. B. Bird, *Molecular Theory of Gases and Liquids* (Wiley, New York, 1964).
[18]C. Y. Ng, Y. T. Lee, and J. A. Barker, J. Chem. Phys. **61**, 1996 (1974).
[19]G. Scoles, Annu. Rev. Phys. Chem. **31**, 81 (1980).
[20]M. P. Allen and D. J. Tildesley, *Computer Simulation of Liquids* (Clarenden, Oxford, 1987).
[21]S. W. deLeeuw, J. W. Perram, and E. R. Smith, Proc. R. Soc. London A **373**, 27 (1980).
[22]J-P. Hansen, in *Molecular-Dynamics Simulation of Statistical-Mechanical Systems,* Proceedings of the International School of Physics "Enrico Fermi", Course XCVII, Varenna, 1985 (North-Holland, Amsterdam, 1986).
[23]E. R. Cowley, G. Jacucci, M. L. Klein, and I. R. McDonald, Phys. Rev. B **14**, 1758 (1976).
[24]M. Born and K. Huang, *Dynamical Theory of Crystal Lattices* (Oxford University Press, New York, 1954).
[25]E. R. Cowley, S. Satija, and R. Youngblood, Phys. Rev. B **28**, 993 (1983).
[26]A. T. Stewart and B. N. Brockhouse, Rev. Mod. Phys. **30**, 250 (1958).